L-BAND RADAR OBSERVATIONS OF CABEUS CRATER: INITIAL RESULTS FROM DFSAR ONBOARD CHANDRAYAAN-2 MISSION.

S. S. Bhiravarasu[1], T. Chakraborty[1], A. Das[1], R. Kumar[1], C. D. Neish[2], D. K. Pandey[1], G. W. Patterson[3], D. Putrevu[1], and B. J. Thomson[4]. [1]Space Applications Centre (ISRO), Ahmedabad, India (sriram.saran@sac.isro.gov.in), [2]University of Western Ontario, London, ON, Canada, [3]Johns Hopkins University Applied Physics Laboratory, Laurel, MD[3], [4]University of Tennessee, Knoxville, TN.

Introduction: On 9 October 2009 the Lunar Crater Observation and Sensing Satellite (LCROSS) impacted into the floor of the ~101 km diameter Cabeus crater located near the Moon's south pole (85.33°S, 42.13°W). Spectral measurements of the ejecta plume detected the presence of water and hydroxyl along with the presence of a number of other volatile species, including CO_2, light hydrocarbons, ammonia, and sulfur-bearing species [1, 2]. Previous studies using ground-based S-band radar [3] and Mini-RF (LRO) and Mini-SAR (Chandrayaan-1) monostatic radar data [4] of the floor of Cabeus found no evidence for thick deposits of pure water ice within a few meters of the lunar surface. However, recent bistatic S-band observations using the Arecibo observatory and Mini-RF found an opposition surge [5] within a portion of the Cabeus crater floor that is not in permanent shadow, lending support for the presence of blocky, near surface deposits of water ice [6]. Here, we report on the initial observations of the first-ever L-band orbital radar observations of a part of Cabeus' crater floor using DFSAR onboard the Chandrayaan-2 spacecraft

DFSAR background: The Dual Frequency Synthetic Aperture Radar (DFSAR) onboard ISRO's Chandrayaan-2 orbiter is a dual-frequency monostatic system, operating at 24 cm (L band) and 12 cm (S band). DFSAR is capable of acquiring data in full (quad) and hybrid (compact) polarimetry modes, along with standalone (L or S) and simultaneous (L and S) modes of imaging. DFSAR has a selectable slant-range resolution from 2 to 75 m, and acquires data at a wide range of incidence angles (10° to 35°) [7].

Observations: We obtained L-band full-pol (FP) and L- and S-band compact-pol (CP) data of a part of Cabeus crater floor at an incidence angle of 26°. Artifacts present in the S-band CP images of this data rendered it unsuitable for analysis. The FP and CP L-band data sets have an overlap of ~90%, and contain both permanently shadowed (PSR) and sunlit portions of Cabeus' floor but do not cover the LCROSS impact site (**Figure 2**). The slant range resolutions of calibrated, level-1 L-band FP and CP data are 0.5 × 9.6 m, and 0.5 × 19 m in azimuth and range directions respectively. After resampling and terrain correcting the data (for parallax effects) followed by projecting them on to a lunar grid, the final pixel space is 25 m for FP and 45 m for CP data. This yielded a ~50- and 90-look average for each sampled location in FP and CP data with an approximate speckle noise ($1/N^{1/2}$) uncertainty in the Circular Polarization Ratio (CPR) measurements of ± 0.14 and ±0.1 respectively [8]. From the FP and CP data, we derived the CPR using methods described in [4] and [8]. For comparison, we used an S-band Mini-RF controlled CPR mosaic of south pole (~237 m/pixel resolution) produced by the USGS [9]. Using a South Pole LRO LOLA PSR boundary shapefile [10] we extracted mean values for DFSAR L- and Mini-RF monostatic S-band CPR from two PSRs and the surrounding sunlit region on Cabeus' floor, in ArcGIS (**Figure 2**). We selected the sunlit portion based on a region of overlap between the DFSAR FP and CP data. Figure 1 gives the histograms of CPR values obtained from the DFSAR and Mini-RF datasets.

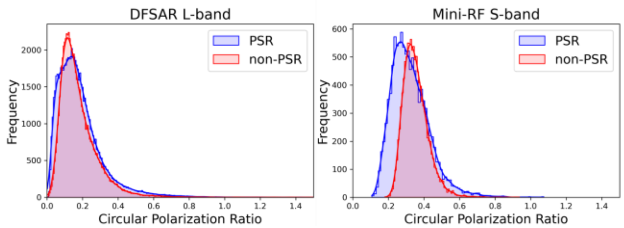

Figure 1: Histograms of circular polarization ratios for PSR and non-PSRs (as outlined in Fig.2) on the floor of Cabeus crater obtained from DFSAR L-band FP (*left*) and Mini-RF monostatic S-band (*right*) data. There is essentially no difference between the radar properties of the sunlit and permanent shadowed portions at either wavelength.

Table 1: Mean CPR values (followed by one standard deviation of the mean) obtained from DFSAR and Mini-RF radar instruments.

Instrument	CPR: PSR	CPR: Non-PSR
L-band DFSAR FP	0.18 ± 0.13	0.18 ± 0.12
L-band DFSAR CP	0.21 ± 0.09	0.15 ± 0.07
S-band Mini-RF	0.32 ± 0.1	0.35 ± 0.08

Results and Discussion: High radar CPR signatures (>1) along with the strong backscatter observed for the Galilean satellites [11] and polar craters on Mercury [12] have been attributed to the presence of water ice in the form of a few to multiple radar wavelengths-thick sheets or slabs. In the case of the Moon, previous works using LRO Diviner temperature measurements indicated that water ice could also be stable within a meter of the surface for widespread regions of polar regions outside of permanent shadow [e.g., 13]. From **Figure 1** and **Table 1**, we observe that the mean CPR values for both the PSR and sunlit portions of Cabeus' crater floor analyzed in this work are less than 0.4.

Moreover, <1% of the pixels in Cabeus crater have L- and S-band CPR values greater than 1. The relatively small increase in the CPR observed at S-band compared to those at L-band are likely a result of the difference in their incidence angle (26° of DFSAR vs ~49° of Mini-RF), with some contributions from differences in wavelength-scale roughness. In addition, we do not observe any differences in the absolute backscatter (co- and cross-polarization channels) from these two regions as observed from DFSAR FP data.

We conclude that: (1) our results are not consistent with the presence of thick, pure water ice deposits within the top ~2-3 meters of the surface in either the PSRs or the sunlit portion of the Cabeus interior analyzed in this work; and (2) the form and quantity of water ice detected in the LCROSS impact ejecta plume [1] is not detectable at L- and S-band radar wavelengths, consistent with the results obtained by [3, 4].

The S-band Mini-RF bistatic observation of Cabeus floor (*2013-127*, outline shown in Figure 2) [6] includes PSRs, but those regions were not analyzed due to the effect of radar shadow noise. However, CPR measurements obtained at grazing incidence angles for the sunlit portions of Cabeus floor show a clear opposition surge [6], for which there is currently no best explanation. This is particularly confounding given that ground-based measurements taken at a similar incidence angle show no such opposition surge [3]. DFSAR data combined with new bistatic measurements of lunar polar regions at a range of incidence and bistatic angles could help us to better understand the radar detection of water ice deposits as well as the differences between monostatic and bistatic radar observations.

References: [1] Colaprete A. et al. (2010) *Science*, *330*(6003), 463–468. [2] Schultz P. H. et al. (2010) *Science*, *330*(6003), 468–472. [3] Campbell D. B. et al. (2006) *Nature*, *443*, 835–837. [4] Neish C. D. et al. (2011) *JGR*, *116*(E01005). [5] Hapke B. and Blewett D. (1991) *Nature*, *352*, 105–117. [6] Patterson G. W. et al. (2017) *Icarus*, *283*, 2–19. [7] Putrevu D. et al. (2016) *Adv. Space Res.*, *57*(2), 627–646. [8] Campbell B. A. (2002) *Cambridge Univ. Press*, Cambridge, U. K. [9] Kirk R. L. et al. (2013) *LPSC XLIII*, Abstract #2920. [10] Mazarico E. et al. (2011) *Icarus*, *211*, 1066–1081. [11] Ostro S. J. et al. (1992) *JGR*, *97*(E11), 18277–18244. [12] Harmon J. K. et al. (2011) *Icarus*, *211*(1), 37–50. [13] Paige D. A. et al. (2010) *Science*, *339*(6117), 300–303.

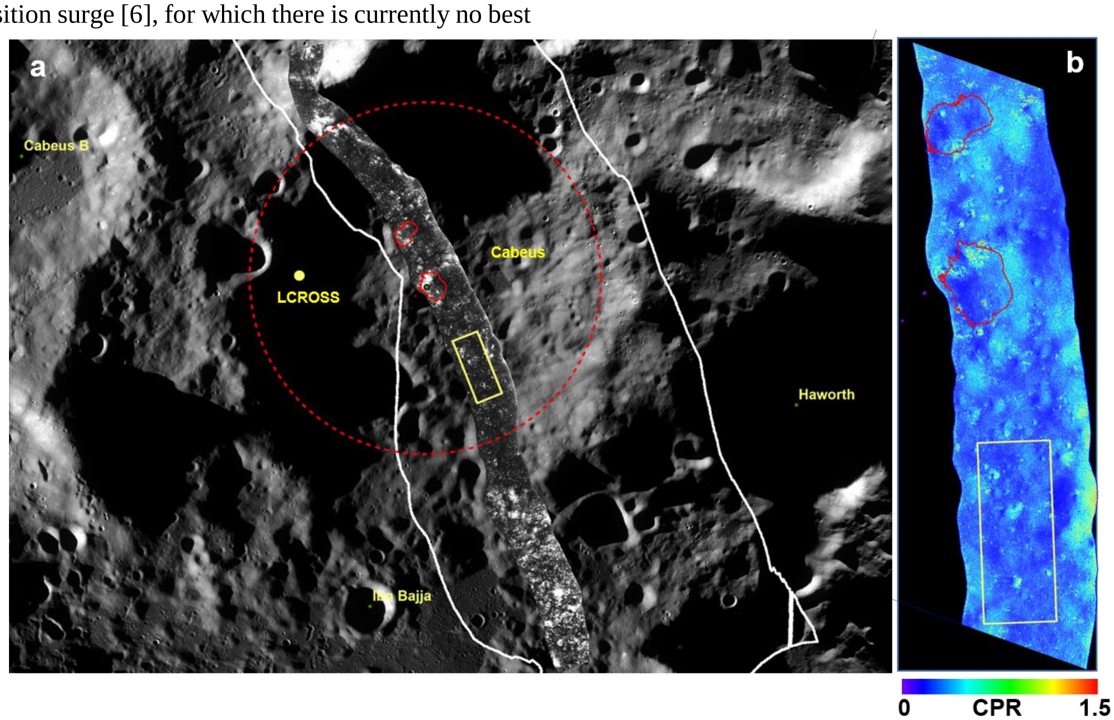

Figure 2: (a) L-band DFSAR HH (Horizontal transmit and receive) polarization image of Cabues crater region overlain on a LROC WAC south pole mosaic. The dashed red circle outlines the inner rim crest of Cabeus crater, the solid yellow dot represents the location of the LCROSS impact, and the white polygon gives the boundaries of Mini-RF bistatic observation *2013-127* analyzed in [6]. The two polygons in red and the yellow box overlain on top of the DFSAR image are PSRs (from LOLA) and a sunlit portion on the floor of Cabeus respectively, from which Figure 1 and values in Table 1 are derived; (b) CPR image derived from the L-band DFSAR FP data shown with PSRs and the sunlit portion as indicated in (a). The CPR is stretched to a color scale and span the color spectrum from purple through red for values between 0 and 1.5. Yellow box and red outlined regions are same as in Fig. 2a.